PET/MRI and Molecular Imaging in Breast Cancer

6

Amy Melsaether, Roy Raad, Thomas Helbich, Linda Moy, and Katja Pinker

6.1 PET/MRI of the Breast

MRI is an indispensable tool in breast imaging with multiple established indications (Sardanelli et al. 2010, 2017; D'Orsi et al. 2013). Dynamic contrast-enhanced MRI (DCE-MRI) is the backbone of any standard MRI breast protocol and the most sensitive method for breast cancer detection with sensitivities ranging up to 98–100%, but variable specificities ranging from 47–97% (Sardanelli et al. 2010; D'Orsi et al. 2013; Pinker et al. 2009; Pinker-Domenig et al. 2012; Morris 2007; Morrow et al. 2011; Mann et al. 2015). The effectiveness of DCE-MRI relies on its ability not only to provide high-resolution morphological information about a given tumor but also functional information about tumor neo-angiogenesis as a cancer specific hallmark. In their multi-step development, cancers acquire several other hallmark capabilities such as proliferative signaling, evading growth suppressors, resisting cell death, enabling replicative immortality and activating invasion and metastasis (Hanahan and Weinberg 2000; 2011). To overcome the limitations of DCE regarding its specificity, multiple other functional MRI parameters such as diffusion-weighted imaging (DWI), proton magnetic spectroscopic imaging (^{1}H-MRSI), phosphorus MRSI, sodium imaging or chemical change saturation transfer imaging (CEST) have been developed and investigated to interrogate more cancer hallmarks in breast imaging, revealing encouraging results (Dorrius et al. 2014; Baltzer et al. 2012; Schmitt et al. 2011; Zaric et al. 2016; Bogner et al. 2009, 2012; Gruber et al. 2011, 2016; Pinker et al. 2012). Despite challenges unique to the individual MRI parameters, some of these parameters, e.g. DWI or ^{1}H-MRSI have been successfully translated from experimental to clinical breast imaging. Their combined application with DCE-MRI is defined as multiparametric MRI (mpMRI) of the breast and data indicate that mpMRI of the breast improves diagnostic accuracy in breast cancer, obviates unnecessary breast

A. Melsaether, M.D. (✉) • R. Raad, M.D.
L. Moy, M.D.
Department of Radiology, NYU Center for Advanced Imaging and Innovation, NYU School of Medicine, New York, NY, USA
e-mail: amy.melsaether@nyumc.org; roy.raad@nyumc.org; linda.moy@nyumc.org

T. Helbich, M.D.
Division of Molecular and Gender Imaging, Department of Biomedical Imaging and Image-guided Therapy, Medical University of Vienna, Vienna, Austria
e-mail: thomas.helbich@meduniwien.ac.at

K. Pinker, M.D., Ph.D., E.B.B.I.
Division of Molecular and Gender Imaging, Department of Biomedical Imaging and Image-guided Therapy, Medical University of Vienna, Vienna, Austria

Department of Radiology, Memorial Sloan Kettering Cancer Center, New York, NY, USA
e-mail: pinkerdk@mskcc.org; katja.pinker-domenig@meduniwien.ac.at

L. Umutlu, K. Herrmann (eds.), *PET/MR Imaging: Current and Emerging Applications*,
https://doi.org/10.1007/978-3-319-69641-6_6

biopsies, and enables an improved assessment and prediction of response to neoadjuvant therapy (Rahbar et al. 2011; Minarikova et al. 2017; Pinker et al. 2013, 2014a, b, 2016; Spick et al. 2014; Rahbar and Partridge 2016; Schmitz et al. 2015; Baltzer et al. 2016; Ei Khouli et al. 2010; Yabuuchi et al. 2008, 2010).

PET is a well-established diagnostic nuclear medicine imaging method that enables the assessment of physiological processes using different radiotracers. However, PET alone provides limited anatomical information and has a low spatial resolution, which results in difficulties in lesion localization and the assessment of potential tumor infiltration into adjacent organs. Therefore, PET is commonly performed in conjunction with other imaging modalities such computed tomography (CT). The most commonly used radiotracer in oncology is [^{18}F]Fluorodeoxyglucose ([^{18}F]FDG). [^{18}F]FDG PET allows the interrogation of another cancer hallmark- reprogramming of energy metabolism- by the assessment of tissue glycolysis, which is typically increased in cancer. In breast imaging [^{18}F]FDG PET/CT has emerged as a valuable tool and is indicated in the local, regional, and axillary staging of locally advanced metastatic or recurrent breast cancer and in the response evaluation of locally advanced and metastatic breast cancer to treatment (Koolen et al. 2012; Moy et al. 2007a; Yutani et al. 1999; Avril and Adler 2007). However, [^{18}F]FDG PET/CT is limited in the detection of small lesions and low grade cancers with sensitivities ranging from 80–87% and specificities ranging from 73–100%, which is inferior to MRI. It is therefore currently not recommended as the method of choice for local staging of known or suspected primary breast malignancies when MRI is available (Samson et al. 2002; Fletcher et al. 2008).

In efforts to combine the advantages of MRI and PET, the concept of PET/MRI has been explored. Several clinical studies evaluated the potential of fused [^{18}F]FDG PET and DCE-MRI for breast cancer diagnosis (Moy et al. 2007a, b, Moy et al. 2010; Garcia-Velloso et al. 2017; Domingues et al. 2009). Moy et al. compared prone [^{18}F]FDG PET and fused [^{18}F]FDG PET/MRI. The authors demonstrated that prone [^{18}F]FDG PET scans were suitable for fusion with DCE-MRI of the breast and increased the confidence of the readers in lesion assessment (Koolen et al. 2012; Yutani et al. 1999; Moy et al. 2007b; Bitencourt et al. 2014a). Domingues et al. investigated fused PET/MRI using [^{18}F]FDG and DCE-MRI and concluded that [^{18}F]FDG PET/MRI provides accurate morphological and functional data for an improved diagnostic accuracy in breast cancer (Domingues et al. 2009). Bitencourt et al. extended the protocol to include DWI for the assessment of breast tumors and reported that mpPET/MRI using three parameters showed good diagnostic accuracy for breast cancer diagnosis (Bitencourt et al. 2014b). To fully exploit the potential of mpPET/MRI, Pinker et al. used a protocol including multiple functional MRI parameters, i.e. DCE-MRI, DWI, ^{1}H-MRSI, and [^{18}F]FDG for the assessment of breast tumors (Pinker et al. 2014b). Mp [^{18}F]FDG PET/MRI provided an improved differentiation of benign and malignant breast tumors when several MRI and PET parameters were combined without missing any cancers (Figs. 6.1 and 6.2). In addition, the authors concluded that [^{18}F]FDG PET/MRI may lead to an up to 50% reduction of unnecessary breast biopsies.

Most recently integrated PET/MRI systems have been developed and introduced into clinical routine. These PET/MRI scanners allow the simultaneous assessment of the multiple hallmark processes in cancer development and progression at multiple levels and therefore can provide a plethora of morphologic, functional, metabolic, and molecular information on breast tumors. To date hybrid PET/MRI data in breast imaging is still scarce. However, initial results for different indications are promising and encourage further research.

6.1.1 Differentiation of Benign and Malignant Breast Tumors

In an initial study Pace et al. compared whole-body [^{18}F]FDG PET/MRI to [^{18}F]FDG PET/CT of the breast and demonstrated that integrated whole-body PET/MRI is feasible in a clinical setting

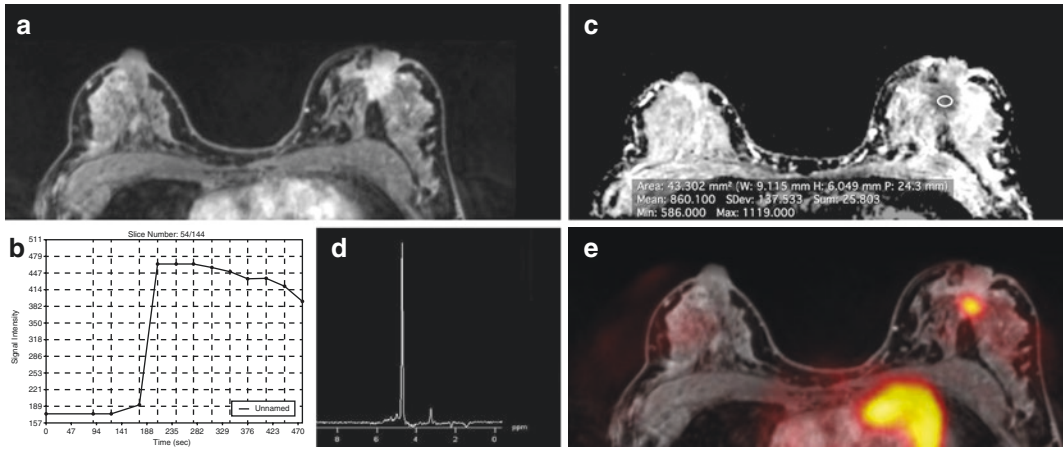

Fig. 6.1 Invasive ductal carcinoma grade 3 (IDC) in the left breast in a 55-year-old woman. The irregular shaped and spiculated mass lesion demonstrates (**a**) initial strong enhancement heterogenous enhancement followed by a wash-out (**b**). DWI shows a restricted diffusivity with low apparent diffusion coefficient (ADC) values (0.86×10^{-3} mm^2/s) (**c**). On proton magnetic resonance spectroscopic imaging, there was a choline peak at 3.2 ppm (dashed arrow) (**d**). The lesion is highly [^{18}F]FDG-avid with an SUVmax of 5.35 further hinting at malignancy (**e**). Multiparametric PET/MRI accurately classified the lesion as BI-RADS 5 (highly suggestive of malignancy)

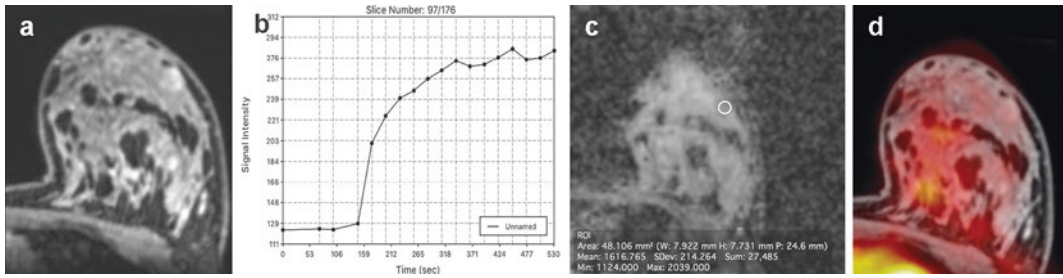

Fig. 6.2 Fibroadenoma in a 39-year-old woman, laterally in the left breast. The slightly irregularly shaped and marginated mass (**a**) demonstrated a heterogeneous medium/persistent contrast enhancement (**b**) and was classified as BI-RADS 4 in DCE-MRI. On diffusion-weighted imaging (DWI), the ADC values (1.616×10^{-3} mm^2/s) (**f**) were well above the threshold for malignancy (**c**) and the lesion is not ^{18}[F]FDG avid (**d**) thus allowing an accurate classification as a benign finding (BI-RADS 3- probably benign) with mp [^{18}F]FDG PET/MRI

with high quality and in a short examination time (Pace et al. 2014). Botsikas investigated sequential [^{18}F]FDG PET/MRI for the detection and primary staging of breast cancer (Botsikas et al. 2016). In a sequential PET/ MRI system, the MRI and the PET are located in the same room at a certain distance and share a common rotating table. The patient is first scanned on one device (MRI), after which the table rotates and the patient is scanned on the second device (PET). This approach also allows PET/MRI the acquisition of automatically co-registered sequentially acquired PET and MR images. In this study the authors reported areas under the curve (AUC) for breast cancer detection of 0.9558, 0.8347 and 0.8855 with MRI, qualitative and quantitative [^{18}F]FDG PET/MRI, respectively ($p = 0.066$). The specificity for MRI and [^{18}F]FDG PET/MRI for primary cancers was 67 and 100% ($p = 0.03$) and for lymph nodes 98% and 100% ($p = 0.25$). The authors conclude that in breast cancer patients, MRI alone has the highest diagnostic accuracy for primary tumors, yet for the assessment of nodal metastases both MRI and [^{18}F]FDG PET/MRI are highly specific.

Jena et al. focused on the reliability of pharmacokinetic DCE-MRI parameters (Ktrans, Kep, ve) derived as part of a routine high resolution

breast MRI protocol when using a simultaneous [18F]FDG PET/MRI system for the differentiation of benign and malignant lesions. The results suggest that a reliable measurement of pharmacokinetic parameters with reduced acquisition time is feasible. In this study receiver operating characteristic (ROC) curve analysis revealed a cut off value for Ktrans, Kep, ve as 0.50, 2.59, 0.15 respectively, which reliably distinguished benign and malignant breast lesions. There was an overall diagnostic accuracy of 94.50%, 79.82% and 87.16% for Ktrans, Kep, ve respectively. The introduction of native T1 normalization with an externally placed phantom enabled a higher accuracy than without native T1 normalization (93.50% vs. 94.50%) with an increase in specificity of 87% vs. 84% (Jena et al. 2017).

6.1.2 Primary Staging of Breast Cancer

Tanjea et al. assessed the utility of [18F]FDG PET/MRI in the initial staging of breast carcinoma (Taneja et al. 2014). In this study 36 patients with breast cancer underwent dedicated breast primary and nodal as well as whole body staging (Fig. 6.3). The study showed a sensitivity

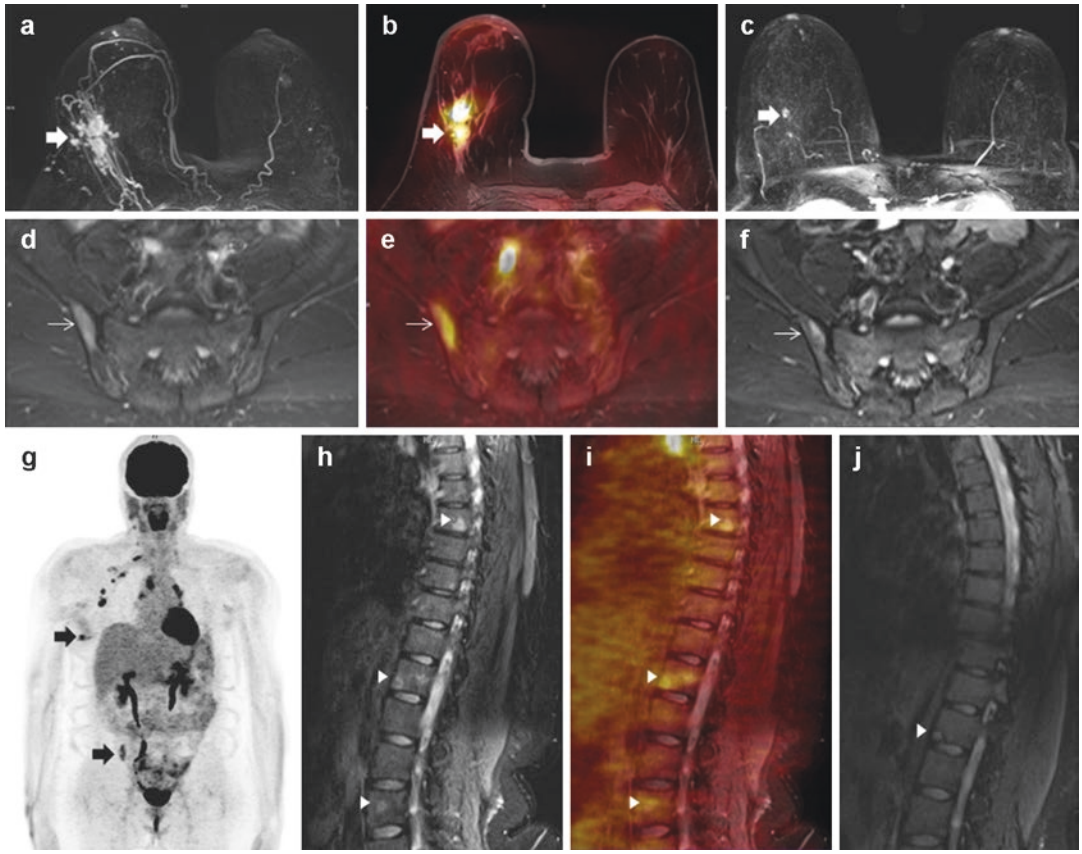

Fig. 6.3 Invasive ductal cancer in the right breast (thick arrows). 1 min subtraction MIP image (**a**) [18F]FDG PET/MRI fused axial (**b**) show a metabolically active mass with satellite lesions. STIR axial (**d**) and [18F]FDG PET/MRI fused axial (**e**) showing [18F]FDG avid marrow lesion in the right iliac bone (thin arrows in (**d**) and (**e**)). [18F]FDG PET/MRI MIP image (**g**) shows multiple focal hypermetabolic areas (thick arrows). STIR sagittal (**h**) and [18F]FDG PET/MRI fused sagittal (**i**) show multiple mildly [18F]FDG avid marrow lesions in vertebrae (arrow heads). 1 min subtraction MIP image (**c**) STIR axial (**f**) and STIR sagittal (**j**) show marked regression of primary breast as well as osseous lesions after chemotherapy. *Reprinted with permission from:* Taneja S, Jena A, Goel R, Sarin R, Kaul S. Simultaneous whole-body 18F-FDG PET-MRI in primary staging of breast cancer: a pilot study. Eur J Radiol. 2014;83(12):2231–9

of 60% and 93.3% for PET and MRI. In the detection of axillary lymph nodes metastases there was a specificity of 91% for both and a false-negative rate of 6.7% on MRI and 40% on [^{18}F]FDG PET. [^{18}F]FDG PET/MRI increased diagnostic confidence for nodal involvement. Distant metastases were found in 22% of patients at the time of diagnosis. Overall [^{18}F]FDG PET/MRI led to a change in management in 12 (33.3%) patients. The authors conclude that in this pilot study simultaneous [^{18}F]FDG PET/MRI has been useful in whole-body initial staging of breast cancer patients. Eun-Jung Kong et al. investigated the application of combined whole-body and dedicated [^{18}F]FDG PET/MRI of the breast in 42 breast cancer patients (Kong et al. 2014). They authors conclude that such a "one-stop-shopping" examination is feasible and facilitates the benefits of combining high-resolution local breast and whole-body staging with metabolic images. They found that [^{18}F]FDG breast PET/MRI utilizing a dedicated coil is still necessary to enable an accurate diagnosis and staging of invasive carcinomas that are less than 1 cm in size.

6.1.3 Assessment of Tumor Aggressiveness

Margolis et al. investigated the feasibility of dedicated [^{18}F]FDG PET/MRI of the breast to assess the synergy of MR pharmacokinetic and [^{18}F]FDG uptake data to determine tumor aggressiveness in terms of metastatic burden and Ki67 status (Fig. 6.4) (Margolis et al. 2016). In this study patients with systemic metastases showed significantly lower kep values compared to patients with local disease (0.45 vs. 0.99 min^{-1}, $p = 0.011$). Metastatic burden was positively correlated with Ktrans and standardized uptake values (SUV), and negatively with kep. Ki67 positive tumors showed a significantly greater Ktrans compared to Ki67 negative tumors (0.29 vs. 0.45 min^{-1}, $p = 0.03$). These preliminary data suggest that MRI pharmacokinetic and [^{18}F]FDG PET parameters may aid in the assessment of tumor aggressiveness and metastatic potential.

6.1.4 Therapy Monitoring

In a case-report study of four patients with locally advanced breast cancer, Romeo et al. evaluated the response to neoadjuvant cytotoxic and endocrine therapy with mp [^{18}F]FDG PET/MRI using DCE-MRI with pharmacokinetic modelling, DWI and maximum standard up-take values (SUVmax) (Romeo et al. 2017) (Fig. 6.5). Therapy monitoring in both types of neoadjuvant treatment with mp [^{18}F]FDG PET/MRI was successfully performed and the authors conclude another potential application for [^{18}F]FDG PET/MRI in breast cancer care might be the concurrent evaluation of breast tumor extension, nodal involvement, for the detection of distant metastasis, and for treatment monitoring.

6.1.5 Breast Cancer Recurrence

Grueneisen et al. investigated whole-body mp [^{18}F]FDG PET/MRI for the detection of local, regional and distant recurrences of breast cancer (Grueneisen et al. 2017). mpPET/MRI readings showed a significantly higher accuracy and higher confidence levels for the detection of recurrent breast cancer lesions when compared to MRI alone ($p < 0.05$). Although for the detection of local recurrences dedicated mpMRI of the breast is most likely sufficient, combined whole body and dedicated [^{18}F]FDG PET/MRI of the breast has an inherent benefit of simultaneous accurate regional and distant staging.

6.1.6 Future Developments and Potential Applications: Specific Radiotracers

PET/MRI of the breast is currently mainly performed using the radiotracer [^{18}F]FDG. [^{18}F]FDG is a very sensitive, yet not very specific radiotracer and there is a significant overlap in the uptake behavior of benign and malignant lesions. To overcome these limitations, more specific radiotracers to target hallmark processes involved in cancer development and progression are continuously being

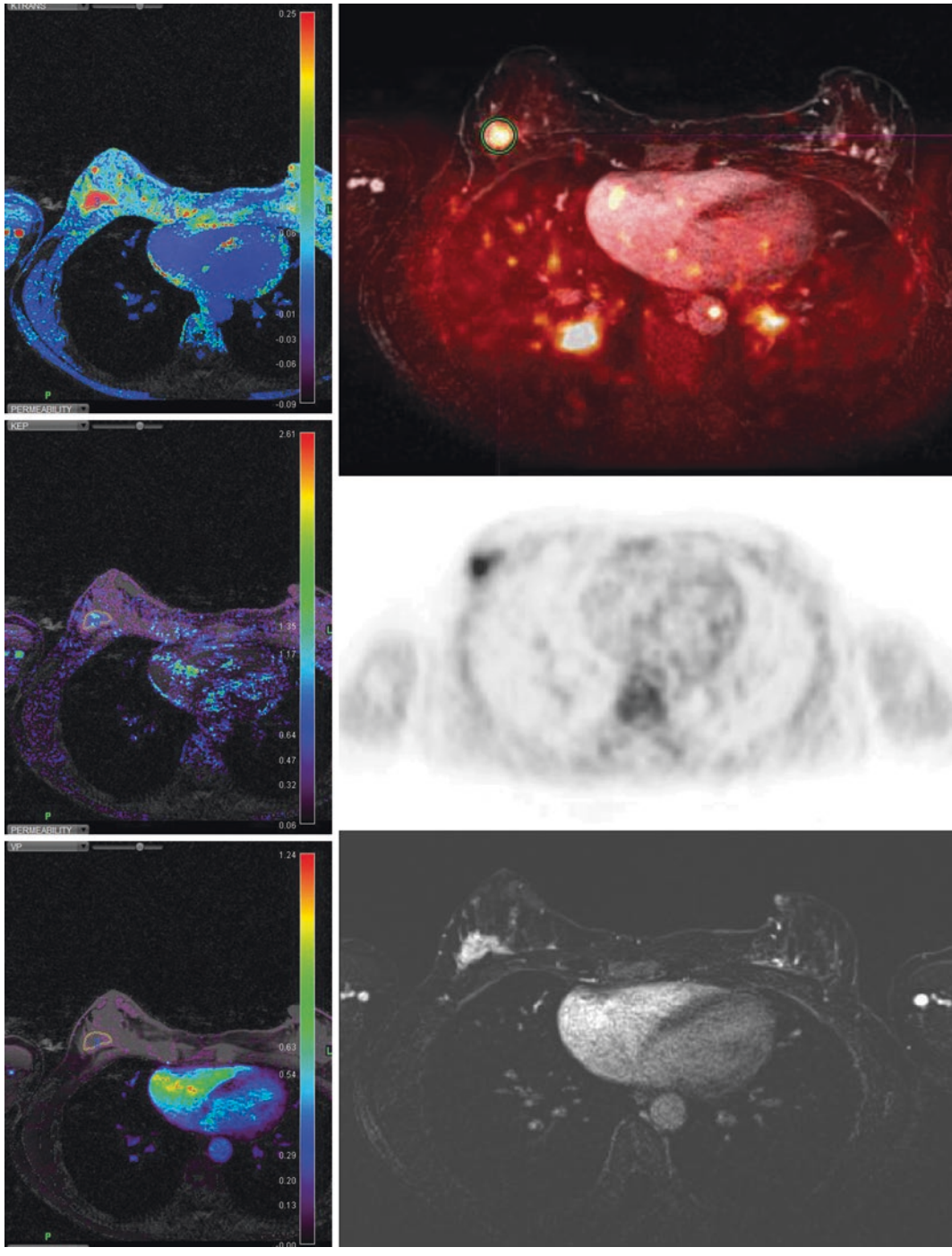

Fig. 6.4 39 year old female with ER, PR, and HER2 positive right breast cancer. Left top to bottom: MR PET Fusion, PET, and MR axial radial VIBE images. Right top to bottom: Ktrans, KEP, and VP color maps. Regions of interest have been drawn over the enhancing area of the tumor as depicted by the radial VIBE sequence *Reprinted with permission from*: Margolis NE, Moy L, Sigmund EE et al. Assessment of aggressiveness of breast cancer using simultaneous 18F-FDG-PET and DCE-MRI: preliminary observation. Clin Nucl Med. 2016;41(8):e355–61

developed such as ^{18}F-fluorodeoxythymidine ([^{18}F]FLT) and ^{18}F-deoxyfluoroarabinofuranosylthymine ([^{18}F]FMAU) for DNA synthesis and cell proliferation; [^{18}F-fluoromisonidazole ([^{18}F]FMISO) for the assessment of tumor hypoxia, or ^{18}F-fluoroestradiol ([^{18}F]FES) or ^{18}F-fluorodihydrotestosterone ([^{18}F]FDHT) for the assessment of receptor status and are also being investigated for breast imaging:

Although these specific radiotracers currently play a greater role in whole body staging and therapy monitoring of advanced breast cancer, their application has also been investigated for primary breast lesions. A promising application seems to be the assessment of tumor hypoxia as one of the most pervasive tumor microenvironmental factors and a feature of most solid tumors (Grueneisen et al. 2017). Conclusive research has shown that tumor hypoxia is one of the key factors in inducing the development of cell clones with an aggressive and treatment-resistant phenotype that leads

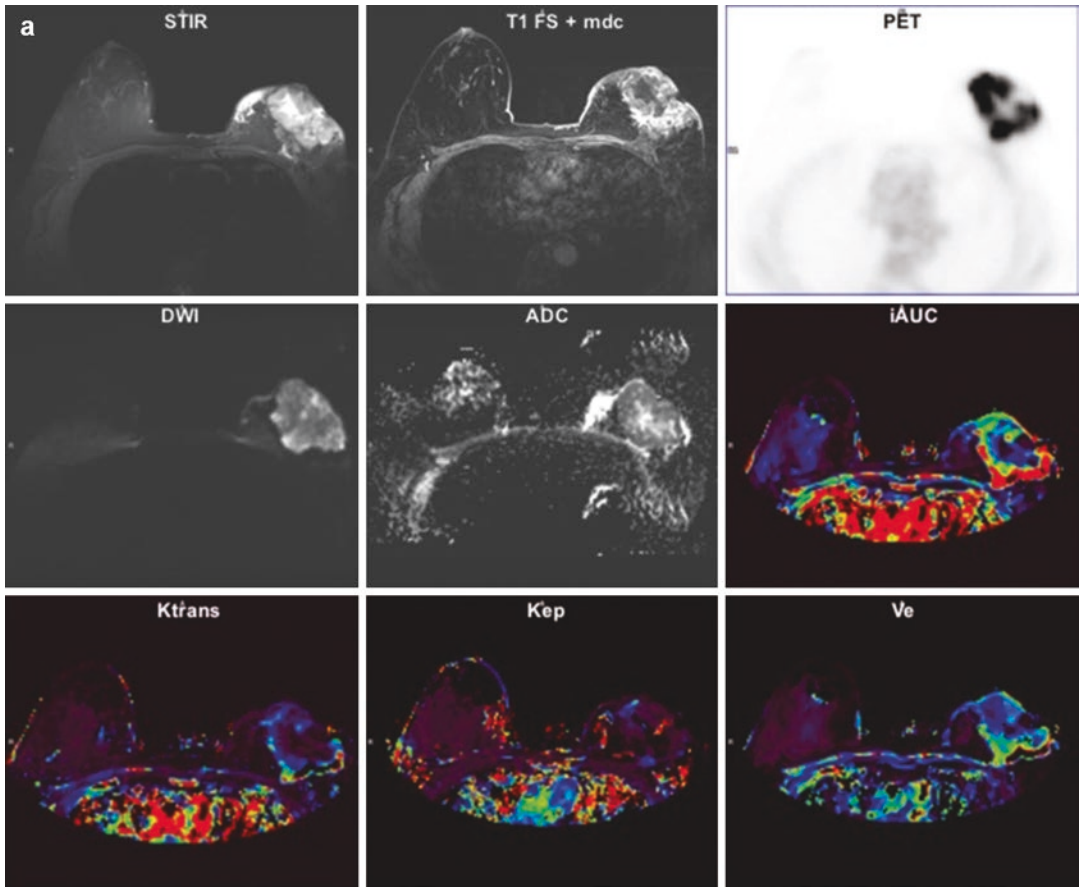

Fig. 6.5 (**a**) Invasive ductal/lobular cancer in a 54-year old female. Multiparametric evaluation of morphological (STIR and DCE), metabolic (PET) and functional (DWI, ADC, iAUC, Ktrans, kep, Ve) parameters before cytotoxic chemotherapy. A large tumoral mass with significant post-contrast enhancement, increased of [^{18}F]FDG uptake, restricted diffusivity and increased perfusion is appreciated. (**b**) Multiparametric evaluation of morphological (STIR and DCE), metabolic (PET) and functional (DWI, ADC, iAUC, Ktrans, kep, Ve) parameters after the second cycle of cytotoxic chemotherapy. A significant reduction of tumor volume, [^{18}F]FDG, perfusion and an increased diffusivity are now detected compared to the pre-treatment evaluation. *Reprinted with permission from:* Romeo V, D'Aiuto M, Frasci G, Imbriaco M, Nicolai E. Simultaneous PET/MRI assessment of response to cytotoxic and hormone neo-adjuvant chemotherapy in breast cancer: a preliminary report. Med Oncol. 2017;34(2):18

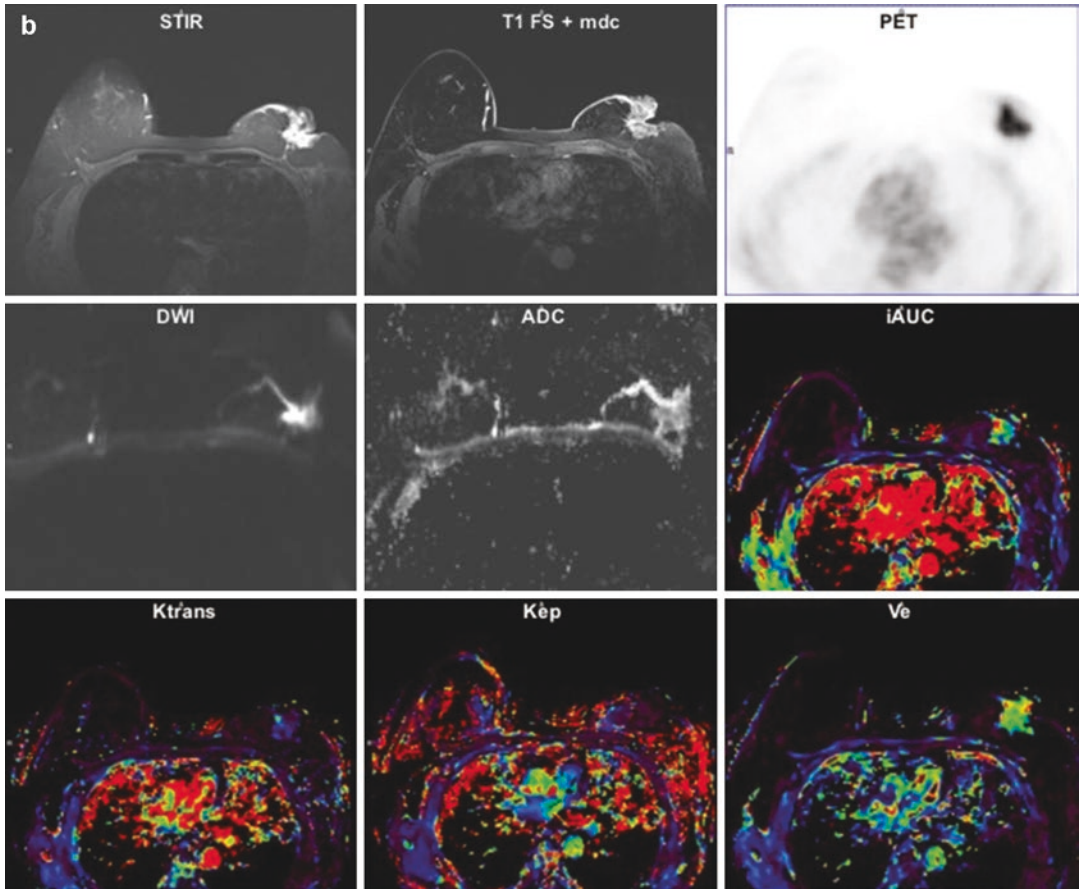

Fig. 6.5 (continued)

to rapid progression and a poor prognosis (Ruan et al. 2009; Vaupel 2008; Hockel et al. 1996a, b; Hockel and Vaupel 2001a, b; Okunieff et al. 2003; Tatum et al. 2006; Vaupel et al. 2002). The radiotracer [^{18}F]FMISO has a high affinity to hypoxic cells with active nitroreductase enzymes and accumulates in activated tumor cells, but not necrotic cells. Cheng et al. investigated whether [^{18}F]FMISO PET/CT can predict primary resistance to endocrine therapy in estrogen-receptor-positive breast cancer, and found a significantly positive correlation between baseline [^{18}F]FMISO uptake and clinical outcomes after ≥3 months of primary endocrine therapy with letrozole. These preliminary results indicate that [^{18}F]FMISO PET/CT may be an effective method for early monitoring of response to neo-endocrine therapy (Cheng et al. 2013). In a recent feasibility study, Pinker et al. investigated fused mp PET/MRI of breast tumors with DCE-MRI, DWI, [^{18}F]FDG, and [^{18}F]FMISO in eight patients (Fig. 6.6). MRI and PET parameters were correlated with pathological features, grading, proliferation-rate (ki67), immuno-histochemistry, and the clinical endpoints: metastasis and death (Pinker et al. 2015). There were several moderate-to-excellent correlations between quantitative imaging markers, grading, receptor status, and proliferation rate. DCE-MRI, [^{18}F]FDG-, and [^{18}F]FMISO-avidity strongly correlated with the presence of metastases [$r = 0.75$ ($p < 0.01$), 0.63 ($p = 0.212$), and 0.58 ($p = 0.093$)], and patients' death [$r = 0.60$ ($p = 0.09$), 0.62 ($p = 0.08$), 0.56 ($p = 0.11$)]. These initial data suggest that mp[^{18}F]FDG /[^{18}F]FMISO PET/MRI might be able to provide quantitative prognostic information in breast cancer patients.

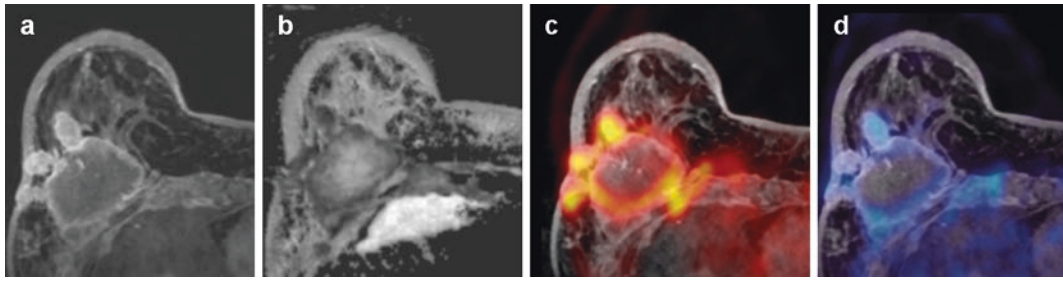

Fig. 6.6 Invasive ductal carcinoma triple-negative grade 3 (IDC) with ki-67 90% in the right breast in a 70-year-old woman. The irregular shaped and marginated mass lesion demonstrates (**a**) a strong enhancement rim with central necrosis and several satellite nodules in the immediate vicinity. DWI shows a restricted diffusivity with low apparent diffusion coefficient (ADC) values (0.665×10^{-3} mm^2/s) (**b**). The enhancing part of the lesion and especially the satellites are highly [^{18}F]FDG-avid indicating increased tissue glycolysis (**c**) and ^{18}[F]MISO-avid indicating tumor hypoxia as a prognostic bad indicator (**d**)

In summary, mpPET/MRI of the breast with different functional MRI parameters visualizes and quantifies processes of cancer development and progression at multiple levels, and provides specific information about the hallmarks of cancer. Initial results indicate that mp[^{18}F]FDG-, PET/MRI of the breast can improve diagnostic accuracy in breast cancer and obviate unnecessary breast biopsies. It can be expected that in the future the role of PET/MRI will further increase through application of specific radiotracers and that it might play a major role as part of precision medicine in breast cancer.

6.2 Molecular Breast Imaging Tools BSGI and PEM

Two molecular breast imaging tools—breast-specific gamma imaging (BSGI)/molecular breast imaging (MBI) and positron emission mammography (PEM) have been introduced recently. Both exams use dedicated breast-specific gamma technology to detect increased blood flow to cancerous cells in the breasts. While BSGI/MBI is based on the assessment of Tc-99 m sestamibi uptake, PEM uses F18-fluorodeoxyglucose (FDG). The benefit of both exams is that they have a higher spatial resolution than PET/CT and may detect small breast tumors that are below the resolution of conventional PET equipment. A drawback is that these imaging studies do not evaluate anatomy. Hence, they differ from conventional breast imaging studies such as mammography, ultrasound and MRI, where the anatomy is clearly depicted. Another limitation is that both tests only facilitate local staging of the breast and axilla and do not enable assessment of distant metastases.

One of the commercially available BSGI systems, the Dilon 6800 system (Dilon Technologies, Newport News, Va), uses a single 15 × 20-cm detector plate composed of an array of 3 × 3-mm sodium iodide crystals. Similar to mammography, the breast is compressed between the detector plate and a compression paddle. The images obtained are in projections similar to conventional mammographic views. PEM uses a pair of dedicated gamma radiation detectors placed above and below the breast and mild breast compression to detect coincident gamma rays after administration of 18F-FDG.

Small single center studies have compared BSGI to mammography in asymptomatic high risk women with dense breasts in the screening setting. They found that BSGI detects mammographically occult breast cancers and is unaffected by dense breast tissue, a major drawback of conventional mammography (Brem et al. 2002, 2005, 2008; Rechtman et al. 2014). Rhodes et al. demonstrated that BSGI had a breast cancer detection rate three times that of mammography (9.6 per 1000 vs. 3.2 per 1000) when a dose of 740 MBq (20 mCi) of 99mTc-sestamibi was injected (Rhodes et al. 2011). However, there are concerns about the radiation risk from BSGI as a

screening tool (Hendrick and Tredennick 2016). In 2015, Rhodes published a follow up study where a lower dose of 300 MBq (8 mCi) was used. The results revealed a higher cancer detection rate of BSGI (10.7 per 1000) compared to mammography alone (3.2 per 1000) despite using a lower dose (Rhodes et al. 2015). The cancer detection rate for mammography combined with BSGI was 12.0 per 1000 (Rhodes et al. 2015). Additional studies are necessary to determine if the reduced-dose BSGI may be an appropriate supplemental breast cancer screening tool in women with dense breasts given the radiation risk (Hendrick and Tredennick 2016). Comparable to BSGI systems, PEM is also commercially available. However, the clinical utility of PEM has yet to be demonstrated, restricting its successful establishment into clinical imaging.

6.3 Whole Body PET/MRI in Breast Cancer

PET/MRI is particularly exciting in the context of whole body imaging for breast cancer patients, facilitating a single, thorough exam with high sensitivity in typical sites of metastasis. At present, there is no uniform recommendation for body imaging in newly diagnosed breast cancer patients. If performed, body imaging is non-standardized and may consist of a PET/CT or of a mix of radionuclide bone scan, chest radiograph, abdominal and pelvic CT, and brain MRI, depending on a patient's symptoms. Notably, in patients with breast cancers 2 cm or greater, whole body imaging has been shown to detect clinically occult distant metastases in approximately 6–10% of patients (Bernsdorf et al. 2012; Groheux et al. 2008) and clinically occult non-axillary nodal metastases in up to 22% of patients (Taneja et al. 2014; Groheux et al. 2008). Detection of early, still isolated organ metastases, especially in the brain and liver, is important because local treatment of early metastatic disease has been shown to improve local control and thereby, quality and length of life (Selzner et al. 2000; Mack et al. 2004; Patchell et al. 1990; De Ieso et al. 2015).

Shortcomings that hinder broader implementation of whole body imaging at the time of diagnosis likely include a lack of uniform recommendations and, in case of PET/CT, a relatively high radiation dose of up to approximately 32 mSv. The Lifetime Attributable Risk (LAR) of radiation induced breast cancer due to a single 18FDG-PET/CT has been estimated at up to 0.25%, or 2.5/1000 patients in 30–60 year old women (Huang et al. 2009; Brix et al. 2005). Moreover, PET scans can show high physiologic uptake of FDG in the brain and liver that may obscure underlying lesions (Moon et al. 1998; Gallowitsch et al. 2003).

PET/MRI is a whole body examination that requires significantly less radiation PET/CT (Melsaether et al. 2016) and provides high sensitivity in lymph nodes, bone, liver, and brain via its novel ability to acquire MR data concurrently with metabolic PET data. Early studies specifically in breast cancer patients typically compare PET/MRI with PET/CT and are encouraging, suggesting that replacing CT with MRI does provide some gains in the search for metastatic disease. In general, small studies consistently show that PET/MR detects the same or a few more systemic metastases than PET/CT or PET alone (Pace et al. 2014; Taneja et al. 2014). In assessing bone metastases, Catalano et al. (2015), showed that PET/MRI found not only more osseous metastases, but also more osseous metastases in more patients as compared with PET/CT. One concern is that PET/MRI may miss lung metastases. Raad et al. demonstrated that while PET/MRI did miss small lung nodules in oncologic patients, 97% of the missed nodules were stable at follow-up, suggesting that the missed nodules may be clinically unimportant (Raad et al. 2016). Melsaether et al. found that PET/MRI detected liver, lymph node, bone, and brain metastases not seen on PET/CT. While some of these differences in detection were significant at the lesion level, none reached significance at the patient level, likely because larger patient cohorts would be needed (Melsaether et al. 2016). Finally, Grueneisen et al. looked at PET/MR another way and, rather than comparing PET/MR to PET/CT, showed that adding PET to whole body MR

increases sensitivity and overall accuracy in breast cancer patients (Grueneisen et al. 2017). In that same vein, Heusner et al. demonstrated that adding PET to DWI greatly improves the specificity of DWI in whole body imaging (Heusner et al. 2010).

One of the strengths of PET/MRI is that it is highly customizable. The acquired MR sequences can be varied and adapted accordingly to the request of each of the 6–7 bed positions involving the thighs to the vertex that comprise a PET/MR examination. For example, one could run a T2 weighted post-contrast fluid attenuated inversion recovery (FLAIR) sequence during the brain station to look for leptomeningeal disease and diffusion weighted imaging (DWI) during the liver station in the interest of characterizing liver lesions. Research as to which sequences are the most useful overall and at each station is ongoing. Grueneisen et al. found similar sensitivities for PET combined with MR half-fourier acquisition single-shot turbo spin-echo (HASTE) and DWI, PET combined with MR HASTE and T1-post contrast imaging, and PET combined with MR HASTE, DWI, and T1-post contrast imaging (Grueneisen et al. 2017). They noted that reader confidence was significantly higher when a T1-post contrast sequence was included, as would be expected because of the superior anatomic imaging this sequence provides. Melsaether et al. looked at individual organ systems and found that the post-contrast T1-weighted sequence detected more breast, lung, pleural, and brain metastases (Figs. 6.7 and 6.8) than DWI

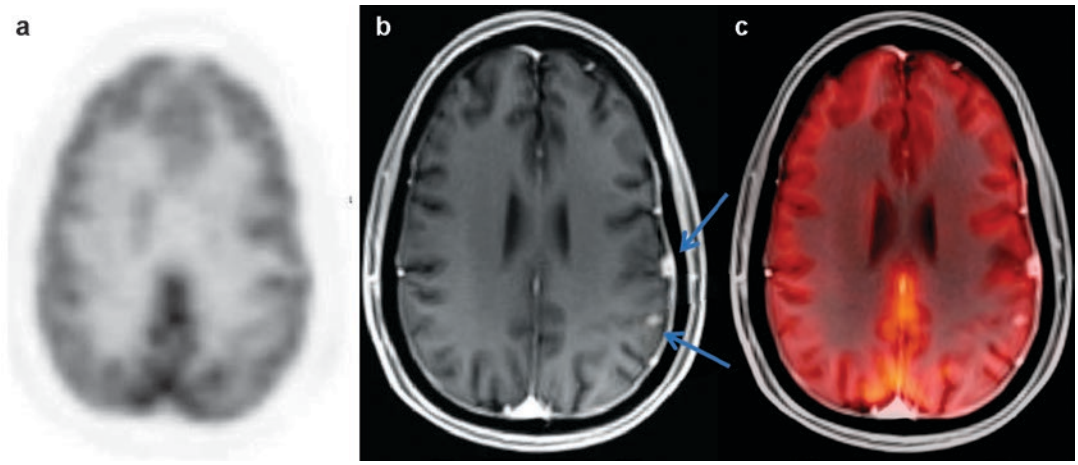

Fig. 6.7 37 year-old female with right breast cancer. An axial PET image (**a**) shows no evidence of metastases while T1 post-contrast (**b**) and fusion (**c**) images demonstrate two adjacent enhancing lesions in the left parietal lobe (arrows), consistent with leptomeningeal metastases

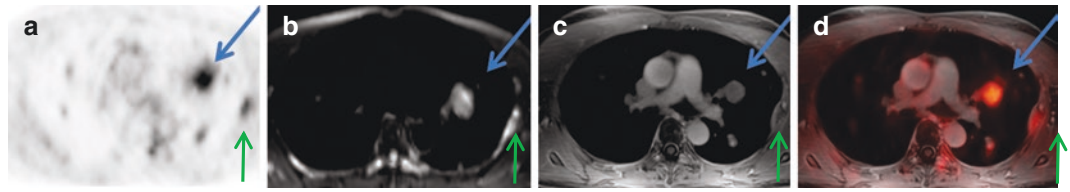

Fig. 6.8 48 year-old female with history of metastatic breast cancer. Axial PET (**a**) , DWI (**b**), T1 post-contrast (**c**), and fusion (**d**) images demonstrate a hypermetabolic 2.5-cm enhancing nodule in the left upper lobe (blue arrow) with restricted diffusion (ADC map not shown), consistent with a lung metastasis. Note the presence of additional lung metastases are best seen on the T1-post-contrast image (**c**), while a hypermetabolic osseous metastasis in a left rib (green arrow), is most conspicuous on the DWI image (**b**)

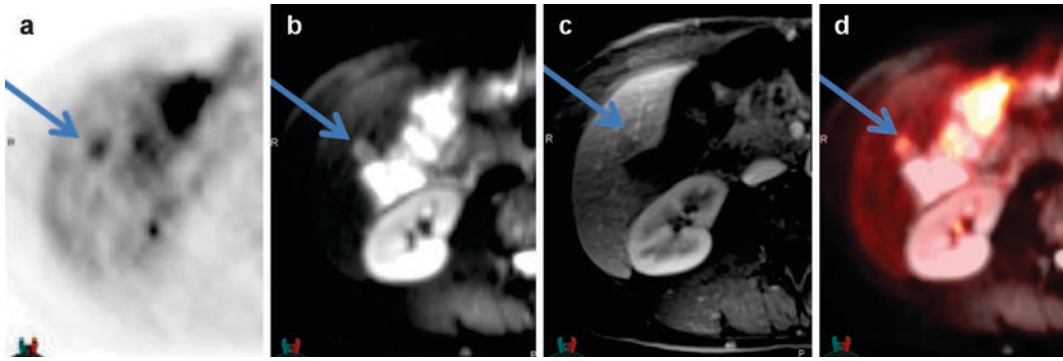

Fig. 6.9 48 year-old female with history of metastatic breast cancer. Axial PET (**a**) and DWI (**b**) images demonstrate a hypermetabolic lesion (**a**) with restricted diffusion (**b**) (ADC map not pictured) in hepatic segment VI (arrow), consistent with a liver metastasis. The lesion is barely visualized on the T1 post-contrast image (**c**), but can be seen on fused images due to increased FDG uptake (**d**)

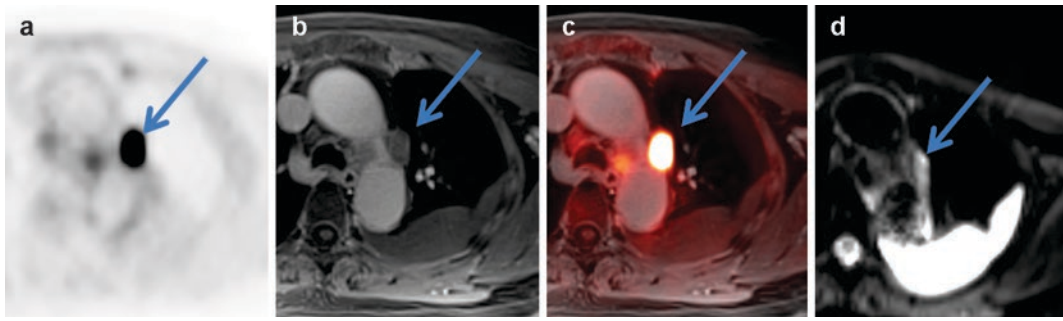

Fig. 6.10 76 year-old female with history of metastatic breast cancer. Axial PET (**a**) , DWI (**b**), Tq post-contrast (**c**) , and fusion (**d**) images demonstrate a hypermetabolic lymph node metastasis in the AP window of the mediastinum (arrow), which is more conspicuous on DWI than on post-contrast T1 imaging. Note the presence of a layering small left pleural effusion

while DWI detected more liver, bone, and nodal lesions than post-contrast T1-weighted imaging (Melsaether et al. 2016) (Figs. 6.9 and 6.10). While the capacity to customize individual stations within a PET/MR examination has not yet been fully explored in the literature, we look forward to what might be on the horizon. Ongoing work will hopefully be able to cut exam time and to improve diagnostic accuracy by finding the most efficient sequences for each station.

In addition to customizing MR sequences, radiotracers beyond ^{18}F-FDG can be administered, either alone or together with ^{18}F-FDG. In breast cancer, ^{18}F-FDG is effective at demonstrating both primary lesions and metastases in any organ because breast cancer cells are typically more metabolically active than surrounding tissue, and, as such, take up and retain more labeled glucose, allowing for lesion detection (Lim et al. 2007). There is some debate as to whether the bone specific radiotracer ^{18}F sodium fluoride (Na-F) outperforms ^{18}F-FDG for detecting osseous metastases, the most common metastases in breast cancer patients. While ^{18}F-NaF imaging finds more osseous lesions, (Piccardo et al. 2015), it is questionable whether lesions seen by ^{18}F-NaF but not by ^{18}F-FDG provide an accurate picture of the disease burden. Specifically, Piccardo et al. (2015) found that no patients with lesions on ^{18}F-NaF, but not ^{18}F-FDG, progressed during their study period and that ^{18}F-FDG parameters, but not ^{18}F-NaF parameters were associated with overall survival. These findings may reflect that ^{18}F-FDG more closely tracks biologically active

breast cancer than does ^{18}F-NaF, whose uptake is tied to osseous blood flow and bony remodeling (Czernin et al. 2010) rather than directly to breast cancer cells.

The next step for functional PET imaging may be to accurately image the characteristics of breast cancer metastases. Primary breast cancers are not uniform throughout. They are heterogeneous, dynamic, and characterized by genomic instability (Marino et al. 2013). In the same way, metastases differ from their index lesion, from one another, and even from themselves over time, especially in response to treatments. Imaging with radio-ligands targeted to molecules that influence therapy would provide a way to non-invasively assess appropriateness of certain therapeutic agents and to reassess when treatment response appears to stall.

Breast cancer biopsy and surgical specimens are commonly assessed histologically for estrogen and progesterone receptors and for human epidermal growth factor receptor 2 (HER2) because these receptors determine whether certain treatments can be effective. Tracers targeting steroid receptors are under development and include the estrogen analog 16a-^{18}F-17B-estradiol (Katzenellenbogen 1995), as well as fluorine labeled progesterone receptor ligands (Gemignani et al. 2013). Zirconium labeled human epidermal growth factor receptor 2 (HER2) receptor tracers including 89Zr-trastuzumab have also been developed (Dijkers et al. 2010; Ulaner et al. 2016). Recently, Ulaner et al. showed that 89Zr-trastuzumab PET can detect HER2 positive metastases in patients with HER2 negative primary breast cancers (Ulaner et al. 2016). This study underlines how functional imaging of metastases, which typically are not biopsied, can provide additional information and potentiate personalized treatment options. Further studies may be able to establish standardized SUV levels that correlate to histologic levels of receptor expression and therapeutic efficacy. Future PET/MRI directions may ultimately include radiolabeled therapies coupled with dynamic PET imaging, which could enable the physician to see in real time whether therapeutic drugs are delivered to and retained within their targets.

References

Avril N, Adler LP. F-18 fluorodeoxyglucose-positron emission tomography imaging for primary breast cancer and loco-regional staging. Radiol Clin N Am. 2007;45(4):645–57. vi

Baltzer PA, Dietzel M, Kaiser WA. MR-spectroscopy at 1.5 tesla and 3 tesla. Useful? A systematic review and meta-analysis. Eur J Radiol. 2012;81(Suppl 1):S6–9.

Baltzer A, Dietzel M, Kaiser CG, Baltzer PA. Combined reading of contrast enhanced and diffusion weighted magnetic resonance imaging by using a simple sum score. Eur Radiol. 2016;26(3):884–91.

Bernsdorf M, Berthelsen AK, Wielenga VT, et al. Preoperative PET/CT in early-stage breast cancer. Ann Oncol. 2012;23(9):2277–82.

Bitencourt AG, Lima EN, Chojniak R, et al. Can 18F-FDG PET improve the evaluation of suspicious breast lesions on MRI? Eur J Radiol. 2014a;83(8):1381–6.

Bitencourt AG, Lima EN, Chojniak R, et al. Multiparametric evaluation of breast lesions using PET-MRI: initial results and future perspectives. Medicine (Baltimore). 2014b;93(22):e115.

Bogner W, Gruber S, Pinker K, et al. Diffusion-weighted MR for differentiation of breast lesions at 3.0 T: how does selection of diffusion protocols affect diagnosis? Radiology. 2009;253(2):341–51.

Bogner W, Pinker-Domenig K, Bickel H, et al. Readout-segmented echo-planar imaging improves the diagnostic performance of diffusion-weighted MR breast examinations at 3.0 T. Radiology. 2012;263(1):64–76.

Botsikas D, Kalovidouri A, Becker M, et al. Clinical utility of 18F-FDG-PET/MR for preoperative breast cancer staging. Eur Radiol. 2016;26(7):2297–307.

Brem RF, Schoonjans JM, Kieper DA, Majewski S, Goodman S, Civelek C. High-resolution scintimammography: a pilot study. J Nucl Med. 2002;43(7):909–15.

Brem RF, Rapelyea JA, Zisman G, et al. Occult breast cancer: scintimammography with high-resolution breast-specific gamma camera in women at high risk for breast cancer. Radiology. 2005;237(1):274–80.

Brem RF, Floerke AC, Rapelyea JA, Teal C, Kelly T, Mathur V. Breast-specific gamma imaging as an adjunct imaging modality for the diagnosis of breast cancer. Radiology. 2008;247(3):651–7.

Brix G, Lechel U, Glatting G, et al. Radiation exposure of patients undergoing whole-body dual-modality 18F-FDG PET/CT examinations. J Nucl Med. 2005;46(4):608–13.

Catalano OA, Nicolai E, Rosen BR, et al. Comparison of CE-FDG-PET/CT with CE-FDG-PET/MR in the evaluation of osseous metastases in breast cancer patients. Br J Cancer. 2015;112:1452–60.

Cheng J, Lei L, Xu J, et al. 18F-fluoromisonidazole PET/CT: a potential tool for predicting primary endocrine therapy resistance in breast cancer. J Nucl Med. 2013;54(3):333–40.

Czernin J, Satyamurthy N, Schiepers C. Molecular mechanisms of bone 18F-NaF deposition. J Nucl Med. 2010;51:1826–9.

D'Orsi CJ, Sickles EA, Mendelson EB, et al. ACR BI-RADS® Atlas, Breast Imaging Reporting and Data System. 5th ed. Reston, VA: American College of Radiology; 2013.

De Ieso PB, Schick U, Rosenfelder N, Mohammed K, Ross GM. Breast cancer brain metastases: a 12 year review of treatment outcomes. Breast. 2015;24(4):426–33.

Dijkers EC, Oude Munnink TH, Kosterink JG, et al. Biodistribution of 89Zr-trastuzumab and PET imaging of HER2-positive lesions in patients with metastatic breast cancer. Clin Pharmacol Ther. 2010;87:586–92.

Domingues RC, Carneiro MP, Lopes FC, da Fonseca LM, Gasparetto EL. Whole-body MRI and FDG PET fused images for evaluation of patients with cancer. AJR Am J Roentgenol. 2009;192(4):1012–20.

Dorrius MD, Dijkstra H, Oudkerk M, Sijens PE. Effect of b value and pre-admission of contrast on diagnostic accuracy of 1.5-T breast DWI: a systematic review and meta-analysis. Eur Radiol. 2014;24(11):2835–47.

Ei Khouli RH, Jacobs MA, Mezban SD, et al. Diffusion-weighted imaging improves the diagnostic accuracy of conventional 3.0-T breast MR imaging. Radiology. 2010;256(1):64–73.

Fletcher JW, Djulbegovic B, Soares HP, et al. Recommendations on the use of 18F-FDG PET in oncology. J Nucl Med. 2008;49(3):480–508.

Gallowitsch HJ, Kresnik E, Gasser J, et al. F-18 fluorodeoxyglucose positron-emission tomography in the diagnosis of tumor recurrence and metastases in the follow-up of patients with breast carcinoma: a comparison to conventional imaging. Investig Radiol. 2003;38(5):250–6.

Garcia-Velloso MJ, Ribelles MJ, Rodriguez M, et al. MRI fused with prone FDG PET/CT improves the primary tumour staging of patients with breast cancer. Eur Radiol. 2017;27(8):3190–8.

Gemignani ML, Patil S, Seshan VE, et al. Feasibility and predictability of perioperative PET and estrogen receptor ligand in patients with invasive breast cancer. J Nucl Med. 2013;54:1697–702.

Groheux D, Moretti JL, Baillet G, et al. Effect of (18) F-FDG PET/CT imaging in patients with clinical Stage II and III breast cancer. Int J Radiat Oncol Biol Phys. 2008;71(3):695–704.

Gruber S, Debski BK, Pinker K, et al. Three-dimensional proton MR spectroscopic imaging at 3 T for the differentiation of benign and malignant breast lesions. Radiology. 2011;261(3):752–61.

Gruber S, Minarikova L, Pinker K, et al. Diffusion-weighted imaging of breast tumours at 3 Tesla and 7 Tesla: a comparison. Eur Radiol. 2016;26(5):1466–73.

Grueneisen J, Sawicki LM, Wetter A, et al. Evaluation of PET and MR datasets in integrated 18F-FDG PET/MRI: a comparison of different MR sequences for whole-body restaging of breast cancer patients. Eur J Radiol. 2017;89:14–9.

Hanahan D, Weinberg RA. The hallmarks of cancer. Cell. 2000;100(1):57–70.

Hanahan D, Weinberg RA. Hallmarks of cancer: the next generation. Cell. 2011;144(5):646–74.

Hendrick RE, Tredennick T. Benefit to Radiation risk of breast-specific gamma imaging compared with mammography in screening asymptomatic women with dense breasts. Radiology. 2016;281(2):583–8.

Heusner TA, Kuemmel S, Koeninger A, et al. Diagnostic value of diffusion-weighted magnetic resonance imaging (DWI) compared to FDG PET/CT for whole-body breast cancer staging. Eur J Nucl Med Mol Imaging. 2010;37:1077–86.

Hockel M, Vaupel P. Biological consequences of tumor hypoxia. Semin Oncol. 2001a;28(2 Suppl 8):36–41.

Hockel M, Vaupel P. Tumor hypoxia: definitions and current clinical, biologic, and molecular aspects. J Natl Cancer Inst. 2001b;93(4):266–76.

Hockel M, Schlenger K, Aral B, Mitze M, Schaffer U, Vaupel P. Association between tumor hypoxia and malignant progression in advanced cancer of the uterine cervix. Cancer Res. 1996a;56(19):4509–15.

Hockel M, Schlenger K, Mitze M, Schaffer U, Vaupel P. Hypoxia and radiation response in human tumors. Semin Radiat Oncol. 1996b;6(1):3–9.

Huang B, Law MW, Khong PL. Whole-body PET/CT scanning: estimation of radiation dose and cancer risk. Radiology. 2009;251(1):166–74.

Jena A, Taneja S, Singh A, Negi P, Mehta SB, Sarin R. Role of pharmacokinetic parameters derived with high temporal resolution DCE MRI using simultaneous PET/MRI system in breast cancer: a feasibility study. Eur J Radiol. 2017;86:261–6.

Katzenellenbogen JA. Designing steroid receptor-based radiotracers to image breast and prostate tumors. J Nucl Med. 1995;36:8S–13S.

Kong EJ, Chun KA, Bom HS, Lee J, Lee SJ, Cho IH. Initial experience of integrated PET/MR mammography in patients with invasive ductal carcinoma. Hell J Nucl Med. 2014;17(3):171–6.

Koolen BB, Vogel WV, Vrancken Peeters MJ, Loo CE, Rutgers EJ, Valdes Olmos RA. Molecular imaging in breast cancer: from whole-body PET/CT to dedicated breast PET. J Oncol. 2012;2012:438647.

Lim HS, Yoon W, Chung TW, Kim JK, Park JG, Kang HK, Bom HS, Yoon JH. FDG PET/CT for the detection and evaluation of breast diseases: usefulness and limitations. Radiographics. 2007;27(Suppl 1):S197–213.

Mack MG, Straub R, Eichler K, Söllner O, Lehnert T, Vogl TJ. Breast cancer metastases in liver: laser-induced interstitial thermotherapy—local tumor control rate and survival data. Radiology. 2004;233(2):400–9.

Mann RM, Balleyguier C, Baltzer PA, et al. Breast MRI: EUSOBI recommendations for women's information. Eur Radiol. 2015;25(12):3669–78.

Margolis NE, Moy L, Sigmund EE, et al. Assessment of aggressiveness of breast cancer using simultaneous 18F-FDG-PET and DCE-MRI: preliminary observation. Clin Nucl Med. 2016;41(8):e355–61.

Marino N, Woditschka S, Reed LT, Nakayama J, Mayer M, Wetzel M, Steeg PS. Breast cancer metastasis issues for the personalization of its prevention and treatment. Am J Pathol. 2013;183(4):1084–95.

Melsaether AN, Raad RA, Pujara AC, et al. Comparison of whole-body (18)F FDG PET/MR imaging and whole-body (18)F FDG PET/CT in terms of lesion detection and radiation dose in patients with breast cancer. Radiology. 2016;281(1):193–202.

Minarikova L, Bogner W, Pinker K, et al. Investigating the prediction value of multiparametric magnetic resonance imaging at 3 T in response to neoadjuvant chemotherapy in breast cancer. Eur Radiol. 2017;27(5):1901–11.

Moon DH, Maddahi J, Silverman DH, et al. Accuracy of whole-body fluorine-18-FDG PET for the detection of recurrent or metastatic breast carcinoma. J Nucl Med. 1998;39(3):431–5.

Morris EA. Diagnostic breast MR imaging: current status and future directions. Radiol Clin N Am. 2007;45(5):863–80. vii

Morrow M, Waters J, Morris E. MRI for breast cancer screening, diagnosis, and treatment. Lancet. 2011;378(9805):1804–11.

Moy L, Noz ME, Maguire GQ, et al. Prone mammoPET acquisition improves the ability to fuse MRI and PET breast scans. Clin Nucl Med. 2007a;32(3):194–8.

Moy L, Ponzo F, Noz ME, et al. Improving specificity of breast MRI using prone PET and fused MRI and PET 3D volume datasets. J Nucl Med. 2007b;48(4):528–37.

Moy L, Noz ME, Maguire GQ, et al. Role of fusion of prone FDG-PET and magnetic resonance imaging of the breasts in the evaluation of breast cancer. Breast J. 2010;16(4):369–76.

Okunieff P, Ding I, Vaupel P, Hockel M. Evidence for and against hypoxia as the primary cause of tumor aggressiveness. Adv Exp Med Biol. 2003;510:69–75.

Pace L, Nicolai E, Luongo A, et al. Comparison of whole-body PET/CT and PET/MRI in breast cancer patients: lesion detection and quantitation of 18F-deoxyglucose uptake in lesions and in normal organ tissues. Eur J Radiol. 2014;83(2):289–96.

Patchell RA, Tibbs PA, Walsh JW, et al. A randomized trial of surgery in the treatment of single metastases to the brain. N Engl J Med. 1990;322(8):494–500.

Piccardo A, Puntoni M, Morbelli S, et al. 18F-FDG PET/CT is a prognostic biomarker in patients affected by bone metastases from breast cancer in comparison with 18F-NaF PET/CT. Nuklearmedizin. 2015;54:163–72.

Pinker K, Grabner G, Bogner W, et al. A combined high temporal and high spatial resolution 3 Tesla MR imaging protocol for the assessment of breast lesions: initial results. Investig Radiol. 2009;44(9):553–8.

Pinker K, Stadlbauer A, Bogner W, Gruber S, Helbich TH. Molecular imaging of cancer: MR spectroscopy and beyond. Eur J Radiol. 2012;81(3):566–77.

Pinker K, Bickel H, Helbich T, et al. Combined contrast enhanced magnetic resonance and diffusion weighted imaging reading adapted to the "Breast Imaging Reporting and Data System" for multiparametric 3 T imaging of breast lesions. Eur Radiol. 2013;23(7):1791–802.

Pinker K, Bogner W, Baltzer P, et al. Improved diagnostic accuracy with multiparametric magnetic resonance imaging of the breast using dynamic contrast-enhanced magnetic resonance imaging, diffusion-weighted imaging, and 3-dimensional proton magnetic resonance spectroscopic imaging. Investig Radiol. 2014a;49(6):421–30.

Pinker K, Bogner W, Baltzer P, et al. Improved differentiation of benign and malignant breast tumors with multiparametric 18fluorodeoxyglucose positron emission tomography magnetic resonance imaging: a feasibility study. Clin Cancer Res. 2014b;20(13):3540–9.

Pinker K, Baltzer P, Andrzejewski P, et al. eds. Dual Tracer PET/MRI of Breast Tumors: Insights Into Tumor Biology. In: Archives of The World Molecular Imaging Conference. Honolulu, HI. World Molecular Imaging Society; 2015.

Pinker K, Helbich TH, Morris EA. The potential of multiparametric MRI of the breast. Br J Radiol. 2016:20160715.

Pinker-Domenig K, Bogner W, Gruber S, et al. High resolution MRI of the breast at 3 T: which BI-RADS(R) descriptors are most strongly associated with the diagnosis of breast cancer? Eur Radiol. 2012;22(2):322–30.

Raad RA, Friedman KP, Heacock L, Ponzo F, Melsaether A, Chandarana H. Outcome of small lung nodules missed on hybrid PET/MRI in patients with primary malignancy. J Magn Reson Imaging. 2016;43(2):504–11.

Rahbar H, Partridge SC. Multiparametric MR imaging of breast cancer. Magn Reson Imaging Clin N Am. 2016;24(1):223–38.

Rahbar H, Partridge SC, Eby PR, et al. Characterization of ductal carcinoma in situ on diffusion weighted breast MRI. Eur Radiol. 2011;21(9):2011–9.

Rechtman LR, Lenihan MJ, Lieberman JH, et al. Breast-specific gamma imaging for the detection of breast cancer in dense versus nondense breasts. AJR Am J Roentgenol. 2014;202(2):293–8.

Rhodes DJ, Hruska CB, Phillips SW, Whaley DH, O'Connor MK. Dedicated dual-head gamma imaging for breast cancer screening in women with mammographically dense breasts. Radiology. 2011;258(1):106–18.

Rhodes DJ, Hruska CB, Conners AL, et al. Journal club: molecular breast imaging at reduced radiation dose for supplemental screening in mammographically dense breasts. AJR Am J Roentgenol. 2015;204(2):241–51.

Romeo V, D'Aiuto M, Frasci G, Imbriaco M, Nicolai E, Simultaneous PET. MRI assessment of response to cytotoxic and hormone neo-adjuvant chemotherapy in breast cancer: a preliminary report. Med Oncol. 2017;34(2):18.

Ruan K, Song G, Ouyang G. Role of hypoxia in the hallmarks of human cancer. J Cell Biochem. 2009;107(6):1053–62.

Samson DJ, Flamm CR, Pisano ED, Aronson N. Should FDG PET be used to decide whether a patient with an abnormal mammogram or breast finding at physical examination should undergo biopsy? Acad Radiol. 2002;9(7):773–83.

Sardanelli F, Boetes C, Borisch B, et al. Magnetic resonance imaging of the breast: recommendations from the EUSOMA working group. Eur J Cancer. 2010;46(8):1296–316.

Sardanelli F, Aase HS, Alvarez M, et al. Position paper on screening for breast cancer by the European Society of Breast Imaging (EUSOBI) and 30 national breast radiology bodies from Austria, Belgium, Bosnia and Herzegovina, Bulgaria, Croatia, Czech Republic, Denmark, Estonia, Finland, France, Germany, Greece, Hungary, Iceland, Ireland, Italy, Israel, Lithuania, Moldova, The Netherlands, Norway, Poland, Portugal, Romania, Serbia, Slovakia, Spain, Sweden, Switzerland and Turkey. Eur Radiol. 2017;27(7):2737–43.

Schmitt B, Zamecnik P, Zaiss M, et al. A new contrast in MR mammography by means of chemical exchange saturation transfer (CEST) imaging at 3 Tesla: preliminary results. Rofo. 2011;183(11):1030–6.

Schmitz AM, Veldhuis WB, Menke-Pluijmers MB, et al. Multiparametric MRI with dynamic contrast enhancement, diffusion-weighted imaging, and 31-phosphorus spectroscopy at 7 T for characterization of breast cancer. Investig Radiol. 2015;50(11):766–71.

Selzner M, Morse MA, Vredenburgh JJ, Meyers WC, Clavien PA. Liver metastases from breast cancer: long-term survival after curative resection. Surgery. 2000;127(4):383–9.

Spick C, Pinker-Domenig K, Rudas M, Helbich TH, Baltzer PA. MRI-only lesions: application of diffusion-weighted imaging obviates unnecessary MR-guided breast biopsies. Eur Radiol. 2014;24(6):1204–10.

Taneja S, Jena A, Goel R, Sarin R, Kaul S. Simultaneous whole-body (1)(8)F-FDG PET-MRI in primary staging of breast cancer: a pilot study. Eur J Radiol. 2014;83(12):2231–9.

Tatum JL, Kelloff GJ, Gillies RJ, et al. Hypoxia: importance in tumor biology, noninvasive measurement by imaging, and value of its measurement in the management of cancer therapy. Int J Radiat Biol. 2006;82(10):699–757.

Ulaner GA, Hyman DM, Ross DS, et al. Detection of HER2-positive metastases in patients with HER2-negative primary breast cancer using ^{89}Zr-trastuzumab PET/CT. J Nucl Med. 2016;57(10):1523–8.

Vaupel P. Hypoxia and aggressive tumor phenotype: implications for therapy and prognosis. Oncologist. 2008;13(Suppl 3):21–6.

Vaupel P, Briest S, Hockel M. Hypoxia in breast cancer: pathogenesis, characterization and biological/therapeutic implications. Wien Med Wochenschr. 2002;152(13–14):334–42.

Yabuuchi H, Matsuo Y, Okafuji T, et al. Enhanced mass on contrast-enhanced breast MR imaging: Lesion characterization using combination of dynamic contrast-enhanced and diffusion-weighted MR images. J Magn Reson Imaging. 2008;28(5):1157–65.

Yabuuchi H, Matsuo Y, Kamitani T, et al. Non-mass-like enhancement on contrast-enhanced breast MR imaging: lesion characterization using combination of dynamic contrast-enhanced and diffusion-weighted MR images. Eur J Radiol. 2010;75(1):e126–32.

Yutani K, Tatsumi M, Uehara T, Nishimura T. Effect of patients' being prone during FDG PET for the diagnosis of breast cancer. AJR Am J Roentgenol. 1999;173(5):1337–9.

Zaric O, Pinker K, Zbyn S, et al. Quantitative sodium MR imaging at 7 T: initial results and comparison with diffusion-weighted imaging in patients with breast tumors. Radiology. 2016;280(1):39–48.